Copolymerization Behavior of 7-Methylene-2-methyl-1,5-dithiacyclooctane: Reversible Cross-Propagation

Simon Harrisson and Thomas P. Davis*

School of Chemical Engineering & Industrial Chemistry, University of New South Wales, Sydney, NSW 2052, Australia

Richard A. Evans and Ezio Rizzardo*

CSIRO Molecular Science, Clayton South, VIC 3169, Australia

Received December 4, 2000

ABSTRACT: The copolymerization behavior of 7-methylene-2-methyl-1,5-dithiacyclooctane (MDTO) with a range of common comonomers has been investigated and found to be highly unusual. The resulting copolymers contained blocks of homo-poly(MDTO), even at low MDTO feed ratios. Changes in temperature and monomer concentration have a significant effect on the copolymer composition of methyl methacrylate−MDTO and styrene−MDTO mixtures and therefore on the apparent reactivity ratios. The magnitude of the concentration effect is independent of the solvent. A new copolymerization mechanism is proposed in which the addition of an MDTO radical to the comonomer is reversible while all other propagation reactions are effectively irreversible. To our knowledge, this is the first observation of such a mechanism. Parameters for MDTO−M_2 (M_2 = STY, MMA) according to this model are reported as (r_{MDTO}, r_2, k_{-12}/k_{22}) = (0.06, 7, 17; M_2 = STY) and (0.38, 3.2, 2.5; M_2 = MMA) at 60 °C.

Introduction

The study of free-radical ring-opening polymerization has attracted considerable interest in recent years, as such systems may reduce the shrinkage that accompanies polymerization. A number of reviews have been published on this topic.[1−4] The cyclic allylic sulfide monomers[5−7] undergo complete ring opening under free-radical conditions, to produce high molecular weight polymers. An example of a cyclic allylic sulfide is 7-methylene-2-methyl-1,5-dithiacyclooctane (MDTO, **1**).

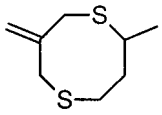

1

This compound polymerizes to complete conversion, to produce a high molecular weight linear polymer that is readily soluble in common organic solvents (Scheme 1). Since the ring-opening step may occur at either of the carbon−sulfur bonds, the polymer formed contains a mixture of two structural units which differ according to the placement of the methyl group, as indicated in Scheme 1.

A common disadvantage of known ring-opening monomers is their low propensity to copolymerize with common monomers such as methyl methacrylate (MMA) and styrene (STY).[8−11] This is due to the low reactivity of the ring-opening monomers' double bonds. In the case of cyclic ketene acetals[8,9] and cyclic vinyl acetals,[12] the double bond resembles that of a vinyl ether; in vinyl cyclopropanes[10,11] and vinyl oxiranes,[13] that of an α-olefin. Attempts to increase the reactivity toward common monomers by the addition of electron-withdrawing substituents[12] have the added effect of stabilizing the first-formed, cyclic radical, with the result that ring opening no longer occurs.

Scheme 1. Ring-Opening Polymerization of 7-Methylene-2-methyl-1,5-dithiacyclooctane (MDTO)

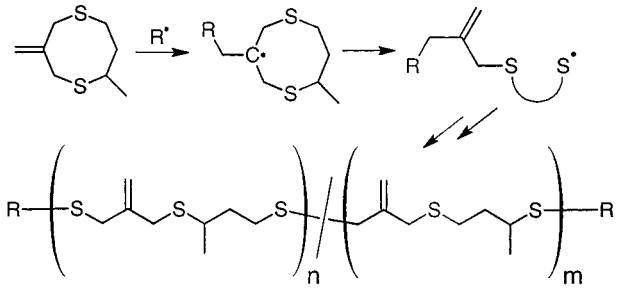

It would be useful, therefore, to find a ring-opening monomer that will readily copolymerize with common monomers. Such a compound might allow the extension of the low-shrink properties of ring-opening monomers to common monomers, resulting in a reduction in the cost of low-shrink materials, and an improvement in their mechanical properties.

This paper describes studies carried out on MDTO (**1**) to determine its reactivity in copolymerizations with common monomers such as MMA, STY, methyl acrylate (MA), and vinyl acetate (VAc). As MDTO shares the basic features of all reported polymerizable cyclic allylic sulfides, we expect that the results reported here will be broadly representative of this class of compounds as a whole.

Experimental Section

Materials. The initiators used were 2,2′-azobis(isobutyronitrile) (AIBN, purchased from TCI-EP) and 1,1′-azobis(cyclohexanenitrile) (VAZO88, purchased from Dupont). AIBN was recrystallized from methanol before use. VAZO88 (98%) was used as received. MMA (99%), STY (99%), MA (99%), and VAc (99%) (obtained from Aldrich) were passed through a

* To whom all correspondence should be addressed.

10.1021/ma0020584 CCC: $20.00
Published on Web 05/11/2001

column of activated basic alumina and then flash-distilled before use. MDTO was synthesized by the method detailed in previous articles.[14,15]

Characterization. ^{1}H and ^{13}C NMR spectra were obtained using a Bruker 200 MHz NMR spectrometer using $CDCl_3$ (Cambridge Isotope Laboratory) as a solvent. Molecular weight data were obtained by GPC (Waters Associates liquid chromatograph) equipped with 10^6, 10^5, 10^4, 10^3, 500, and 100 Å Ultrastyragel columns and a Waters Associates differential refractometer detector. Tetrahydrofuran (flow rate of 1.0 mL/min) was used as eluent. The columns were maintained at 31 °C. The GPC was calibrated with narrow polydispersity polystyrene and poly(methyl methacrylate) standards. A third-order polynomial was used to fit the log M vs time calibration curve. Number molecular weight distributions were derived from the intensity−retention time data, which were processed using KaleidaGraph software.

Procedures. a. Thermal Copolymerizations. General Procedure. The required amounts of monomers and initiator were added to a glass ampule, which was freeze−thaw−degassed and sealed under vacuum. The ampules were immersed in an oil bath controlled to within 0.1 °C of the desired temperature for sufficient time to produce a conversion of less than 10%. The resulting mixture was precipitated with MeOH, and the polymer was dried in a vacuum oven (40 °C) overnight. Conversion was determined gravimetrically. The same procedure was followed for solution copolymerizations except that the components were weighed into a volumetric flask and dissolved in a known volume of solvent. This solution was poured into the ampule. Monomer concentrations in bulk copolymerizations were estimated using known densities of the respective monomers, assuming ideal mixing. Specific examples of a bulk and a solution copolymerization are given below. Experimental details for all thermal copolymerizations may be found in the Supporting Information (Tables S1−S6).

b. Example Copolymerizations. 1. MDTO−MMA, Bulk. AIBN (1.0 mg, 6.1 μmol), MMA (0.8462 g, 8.45 mmol), and MDTO (0.1607 g, 1.67 mmol) were weighed into an ampule, freeze−thaw−degassed, sealed, and immersed in an oil bath heated to 60 ± 0.1 °C for 20 min. Immediately on removal from the bath, the ampule was placed in ice−water to prevent further polymerization, then opened, and its contents precipitated in MeOH. The resulting white powder was dried under vacuum and weighed to determine conversion (22.3 mg, 2.2%). GPC: $M_n = 238 \times 10^3$, PDI = 1.87.

b2. MDTO−STY, 10 wt % in Benzene. AIBN (1.9 mg, 12 μmol), styrene (0.8072 g, 8.36 mmol), and MDTO (0.2909 g, 1.67 mmol) were weighed into a 10 mL volumetric flask, which was subsequently filled with benzene to give a solution containing 1.2 mM AIBN, 0.167 M MDTO, and 0.775 M styrene. This solution was transferred to a glass ampule, freeze−thaw−degassed, sealed, and immersed in an oil bath heated to 60 ± 0.1 °C for 300 min, then removed, and rapidly cooled in an ice−water bath. The ampule was broken open, and hydroquinone (∼1 mg) was added to prevent further polymerization. The benzene was removed under vacuum, and the residue, containing STY−MDTO copolymer, AIBN, hydroquinone, and excess monomers, was dissolved in a small amount of $CHCl_3$ and precipitated into MeOH. The resulting white, powdery precipitate was dried under vacuum and weighed to determine conversion (21.0 mg, 1.92%). GPC: $M_n = 10.0 \times 10^3$, PDI = 1.75.

c. UV-Initiated Copolymerizations. A typical example of a UV-initiated copolymerization follows. STY (0.9136 g, 8.77 mmol), MDTO (0.1005 g, 0.577 mmol), and AIBN (1 mg, 6.1 μmol) were charged to Pyrex sample tubes (10 mm diameter by 60 mm height), deaerated by bubbling with argon for 5 min, and sealed with a rubber septum. The reaction mixture was shaken vigorously before immersion in a constant-temperature bath, in which it was warmed to 25 °C. The sample was then placed in a thermostated copper sample cell and allowed further time to reach thermal equilibrium, before being exposed to pulsed UV laser light at 4 Hz, 15 mJ/pulse. This was produced by a Spectra Physics Quanta-Ray DCR-11 pulsed Nd:YAG laser with a HG-2 harmonic generator, which was used to generate 355 nm UV laser radiation. After 80 min of pulsed laser treatment, the polymerization activity was terminated by adding the reaction mixture to 20 mL of MeOH, thereby precipitating the polymer from its monomer. Conversion was determined gravimetrically to be 2.8% (28.4 mg). GPC: $M_n = 39.8 \times 10^3$, PDI = 5.11.

Further details of the experimental set up used in pulsed laser experiments may be found in one of our earlier publications.[16] Experimental details for all UV-initiated copolymerizations are given in the Supporting Information (Table S7).

d. Copolymer Characterization. The dried copolymers were analyzed by NMR spectroscopy to determine their composition. For all copolymers, MDTO content was determined using the vinylidene hydrogens of the polymer ($\delta \sim 5.0$ ppm, 2H). The styrene content of STY−MDTO copolymers was determined using the aromatic hydrogens of polystyrene (δ 6.2−7.4 ppm, 5H). The MMA content of MMA−MDTO copolymers and the MA content of MA−MDTO copolymers were determined using the OCH_3 resonance (δ 3.5 ppm, 3H). Vinyl acetate content was determined using the acetate CH_3 resonance (δ 2 ppm). Copolymer composition was determined from the relative areas of these resonances, after correcting for the different numbers of hydrogen atoms. A specific example of the characterization of a STY−MDTO copolymer is given below.

e. Copolymer Characterization: Specific Example. A sample of the copolymer prepared in section **b2** was dissolved in $CDCl_3$, and its ^{1}H NMR spectrum was obtained. The ratio of the areas of the aromatic hydrogen resonances (5H) of the styrene groups to the vinylidene hydrogen resonance (2H) from the MDTO repeat units was 53.7:1. The MDTO content of the copolymer was therefore found to be 4.4 mol %.

f. Determination of Reactivity Ratios. Reactivity ratios were determined from the NMR-derived copolymer composition data using nonlinear regression with the Contour program written by Dr. A. M. van Herk.[17] Fits to the three-parameter model developed in this paper were performed using nonlinear regression with the commercially available Kaleidagraph program.

Results and Discussion

Bulk Copolymerizations at 60 °C. Copolymers were produced for the monomerocd pairs MDTO−STY, MDTO−MMA, MDTO−MA, and MDTO−VAc. Compositions of the low-conversion (<10%) copolymers were obtained by NMR spectroscopy. Copolymer composition graphs (bulk, 60 °C) are shown in Figure 1. The solid line in each plot represents the line of best fit to the terminal copolymer composition equation. The reactivity ratios for each monomer pair are given in Table 1. Composition data for each monomer pair, including conversion data, are given in the Supporting Information (Tables S1−S4).

The calculated reactivity ratios show a number of unusual features. The most obvious is that in all cases the product of the two reactivity ratios, r_1r_2, is greater than one. This product represents the degree of deviation from ideal copolymerization, in which $r_1r_2 = 1$. For virtually all radical copolymerizations, $r_1r_2 < 1$,[18] and the monomers show a tendency to alternate. In every copolymerization studied, however, MDTO shows a tendency to form blocks of homopolymer. This tendency has been noted in several other polymerizations where isomerization of the propagating radical occurs, such as cyclopolymerizations[19,20] and the group transfer polymerization of 2-thiocyanatoethyl vinyl ether,[21] and has been attributed to the change in properties of the propagating radical as a result of isomerization.

Another unusual feature of the copolymers is their relatively high MDTO content. MDTO is much more reactive toward styrene and MMA than other ring-

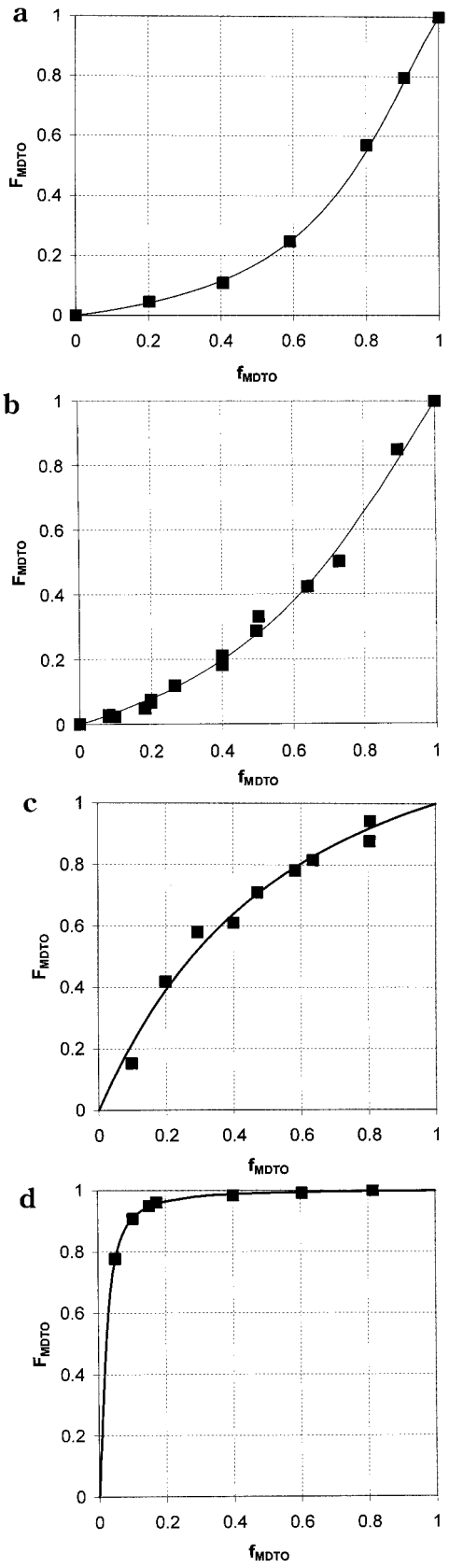

Figure 1. Copolymer composition plots for various comonomers with MDTO. Polymerizations carried out in bulk at 60 °C. (a) STY−MDTO; (b) MMA−MDTO; (c) MA−MDTO; (d) VAc−MDTO.

opening monomers, which have reactivities comparable to that of vinyl acetate. The double bond in MDTO, by contrast, appears to have a reactivity somewhere in between MA and MMA. Structural considerations provide no obvious clue to this enhanced reactivity; MDTO has no substituents that would be expected to activate the double bond to a greater extent than a vinylcyclopropane, for example.

Table 1. Apparent Reactivity Ratios of Monomers in Copolymerization with MDTO at Different Temperatures

M_1[a]	M_2[a]	T (°C)	r_1	r_2	$r_1.r_2$	ref
MDTO	STY	25	0.26	8.6	2.2	this work
MDTO	STY	60	0.52	6.3	3.3	this work
MDTO	STY	80	2.8	13	36	this work
MDTO	MMA	60	0.59	3.1	1.8	this work
MDTO	MMA	80	2.5	4.8	12	this work
MDTO	MA	60	2.8	0.41	1.1	this work
MDTO	VAc	60	140	0.08	11	this work
MDO	STY	*b*	0.021	22.6	0.47	8
MDO	MMA	40	0.057	34.12	1.9	9
VCp1	MMA	60	0.07	11.0	0.77	10
VCp1	STY	60	0.05	17.4	0.87	10
VCp2	MMA	60	0.11	21.49	2.36	11

[a] MDTO: 7-methylene-2-methyl-1,5-dithiacyclooctane; MDO: 2-methylene-1,3-dioxepane; VCp1: 1,1-dichloro-2-vinylcyclopropane; VCp2: 1,1-diethoxycarbonyl-2-vinylcyclopropane; STY: styrene; MMA: methyl methacrylate; MA: methyl acrylate; VAc: vinyl acetate. [b] No temperature reported.

Furthermore, studies on the addition of aromatic thiyl radicals[22,23] and alkyl thiyl radicals[24] to vinyl monomers indicate that the difference in reactivity between styrene and methyl methacrylate should be much greater than what is reported here. Substituted phenylthiyl radicals[22,23] have rates of addition to styrene that are an order of magnitude faster than to methyl methacrylate.

The reactivity ratios obtained from this work suggest, however, that if the terminal model is an accurate description of the copolymerization kinetics, the relative rates of addition of the poly(MDTO) radical to styrene and to methyl methacrylate must be approximately equal. Given the weight of experimental evidence to the contrary it seems that the terminal model does not provide an adequate description of the mechanism of copolymerization of MDTO.

NMR Spectroscopic Analysis of Copolymers. NMR spectra of MDTO-containing copolymers show many of the features of the MDTO homopolymer, even when the MDTO content of the polymer is small. In part, this is due to the length of the MDTO repeat unit, which shields many of the hydrogens from the effect of neighboring comonomer units.

There are, however, several resonances in the spectra of MDTO copolymers that do not appear in the respective homopolymers. In the spectrum of an MMA−MDTO copolymer (Figure 2a), there is a distinctive peak at δ 4.75 ppm, which appears to correspond to the vinylidene proton on an MDTO repeat unit that is cis to a neighboring MMA unit. Similar peaks are seen in MDTO−STY copolymers (Figure 2b). In addition, a new peak (δ 3.65 ppm) is visible slightly downfield of the $-OCH_3$ absorption from polyMMA (δ 3.60 ppm). This is attributed to the $-OCH_3$ moiety on the MDTO−MMA dyad. Likewise, ^{13}C NMR spectra of MDTO−STY or MDTO−MMA copolymers contain only a few peaks that are unique to the copolymer (Figure 3).

The scarcity of new signals suggests that most of the MDTO is present in a similar environment to the homopolymer, that is, in blocks containing two or more MDTO units. This is supported by the presence of fine structure in the quaternary carbon peak at δ 140−142 ppm. The triplet structure is due to long-range interactions between the quaternary carbon and methyl groups

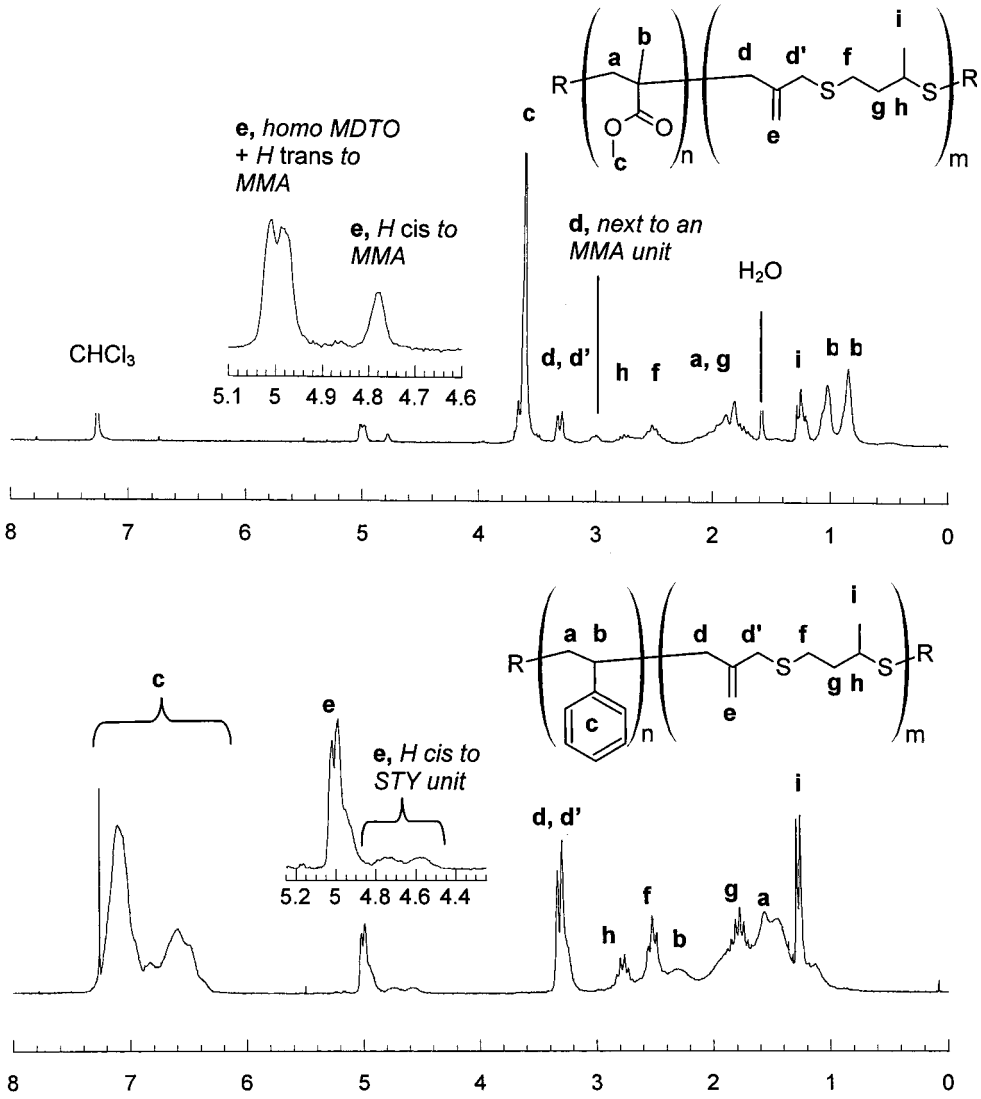

Figure 2. ^{1}H NMR spectra of MDTO copolymers. Expansion shows absorptions due to the vinylidene protons. (a, top) MMA−MDTO (16.3 mol % MDTO); (b, bottom) STY−MDTO (21.6 mol % MDTO).

in neighboring MDTO units[7] and can be seen clearly in Figure 3, even though the mole fraction of MDTO in the copolymer is relatively low (30−40%).

Effect of Temperature. Changes in temperature have a large effect on the composition of MMA−MDTO and STY−MDTO copolymers. Figure 4 shows the effect of temperature on copolymer composition. The best fit reactivity ratios may be found in Table 2.

Such a large temperature effect is unusual in radical polymerizations. For example, there is no significant change in the reactivity ratios for STY−MMA between 40 and 60 °C.[25] This is because the individual propagation reactions have similar, low, activation energies. The presence of a large temperature effect in the copolymerization of MDTO indicates that a reaction with a relatively large activation energy is involved in the mechanism.

New Mechanism. A plausible explanation for these results is that an additional step is involved in the copolymerization mechanism. This step is the reverse of the addition of a polymeric MDTO radical to the comonomer and is represented in Scheme 2. This reaction should have a relatively large activation energy, as it involves the scission of a C−C bond. Therefore, its effect on the copolymer composition should increase with temperature. The existence of such a reaction is plausible, since a nearly identical reaction is observed in allylic sulfide addition−fragmentation chain transfer agents[26] (Scheme 3). The β-scission reaction in these compounds is believed to be very fast, if not instantaneous.[27]

Hence, there are five propagation/depropagation reactions to be considered:

$$M_1^\bullet + M_1 \rightarrow M_1^\bullet \qquad k_{11} \tag{1}$$

$$M_1^\bullet + M_2 \rightarrow M_1M_2^\bullet \qquad k_{12} \tag{2}$$

$$M_1M_2^\bullet \rightarrow M_1 + M_2^\bullet \qquad k_{-12} \tag{3}$$

$$M_2^\bullet + M_1 \rightarrow M_1^\bullet \qquad k_{21} \tag{4}$$

$$M_2^\bullet + M_2 \rightarrow M_2^\bullet \qquad k_{22} \tag{5}$$

We assume that the $M_1M_2^\bullet$ radical shows the same reactivity toward M_1 and M_2 as an $M_2M_2^\bullet$ radical, but only $M_1M_2^\bullet$ radicals are able to depropagate. As $M_2M_2^\bullet$, $M_2M_1^\bullet$, and $M_1M_1^\bullet$ radicals do not depropagate, only reaction 2 is reversible. This differentiates this model from systems involving monomers such as α-methyl-

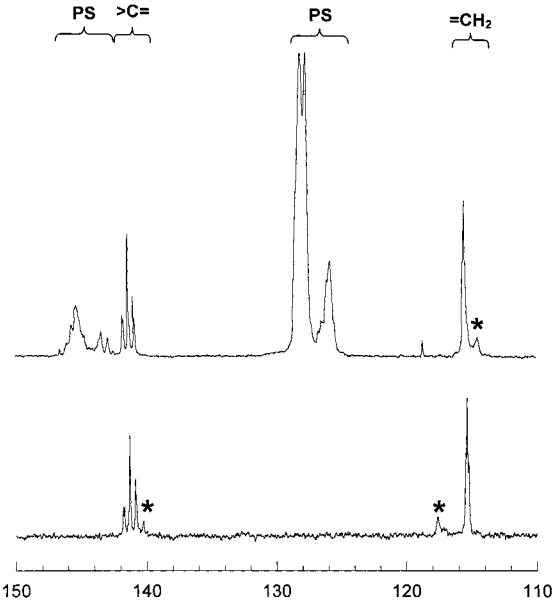

Figure 3. Details from ^{13}C NMR spectra of MDTO copolymers produced in bulk at 80 °C. The fine structure observed in the quaternary carbon peaks is due to interactions with methyl groups in neighboring MDTO groups.[7] Peaks that are unique to the copolymers are marked with an asterisk. (a, top) STY−MDTO (40.7 mol % MDTO); (b, bottom) MMA−MDTO (29.8 mol % MDTO).

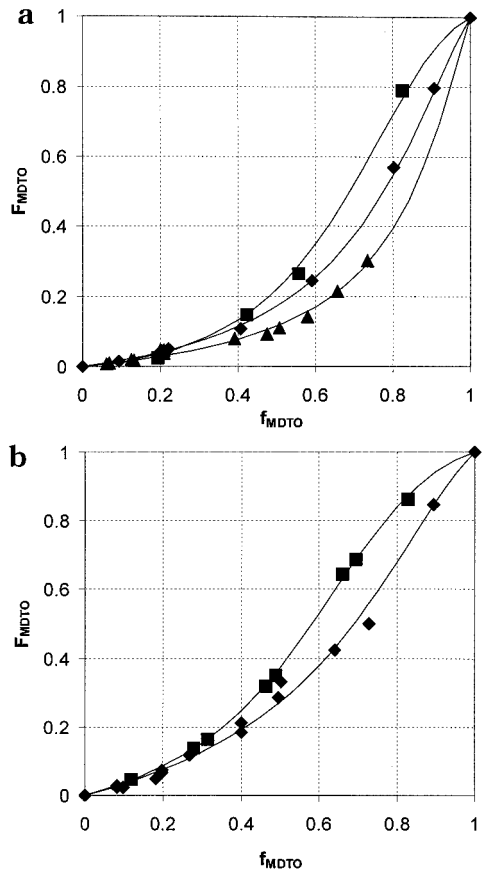

Figure 4. Copolymer composition plot showing the effect of temperature on the copolymer compositions of (a) STY−MDTO and (b) MMA−MDTO. Triangles, 25 °C; diamonds, 60 °C; squares, 80 °C. Solid lines show the values predicted by the reversible cross-propagation model as discussed in the text.

styrene, in which homopropagation reactions are reversible.

Table 2. Parameters for Reversible Cross-Propagation Model in Copolymerizations of MDTO with MMA and STY

comonomer	T (°C)	r_1	r_2	k_{-12}/k_{22}
STY	25	0.061	7	5
	60	0.061	7	17
	80	0.061	7	45
MMA	60	0.38	3.2	2.5
	80	0.38	3.2	10

Scheme 2. Propagation/Depropagation Reactions of the MDTO Radical in Copolymerizations[a]

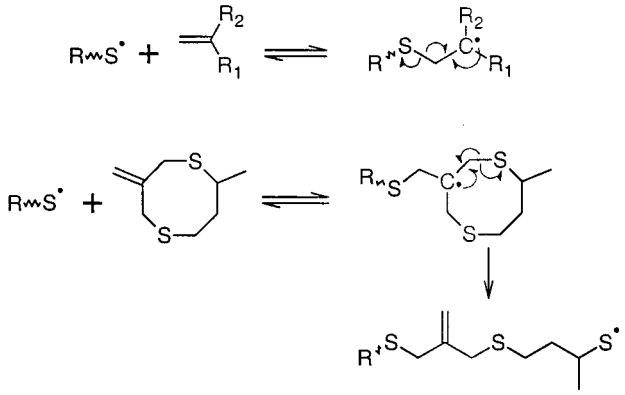

[a] Scission may occur at either C−S bond: for clarity, only one possible scission reaction is shown here.

Scheme 3. Addition Fragmentation Chain Transfer in Allylic Sulfides (Shown: α-(*tert*-Butylthiomethyl)styrene)

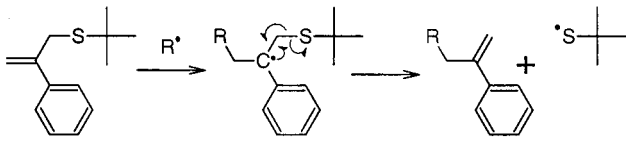

Derivation of the copolymer composition equation in the usual manner produces eq 6a:

$$\frac{d[M_1]}{d[M_2]} = \frac{\langle r_1 \rangle f_1^2 + f_1 f_2}{f_1 f_2 + r_2 f_2^2} \tag{6a}$$

where $\langle r_1 \rangle$ is given by eq 6b:

$$\langle r_1 \rangle = r_1 \frac{f_2 + f_1/r_2 + \dfrac{k_{-12}}{k_{22}([M_1] + [M_2])}}{f_2 + f_1/r_2} \tag{6b}$$

A full derivation of this result can be found in the Appendix.

Equation 6 predicts that the magnitude of the effect will depend on the ratio k_{-12}/k_{22} and on the total monomer concentration. Hence, the largest effects should be seen using comonomers with low homopropagation rate constants and at low concentrations.

The effect of the additional reaction is to produce an increase in the apparent value of r_1. This will result in the observed tendency toward "blockiness".

Other equations associated with the polymerization may be derived in a similar manner. Thus, the expression for the mean sequence length of M_1 units is given by eq 7:

$$\bar{n}_1 = 1 + 2\langle r_1 \rangle \frac{f_1}{f_2} \tag{7}$$

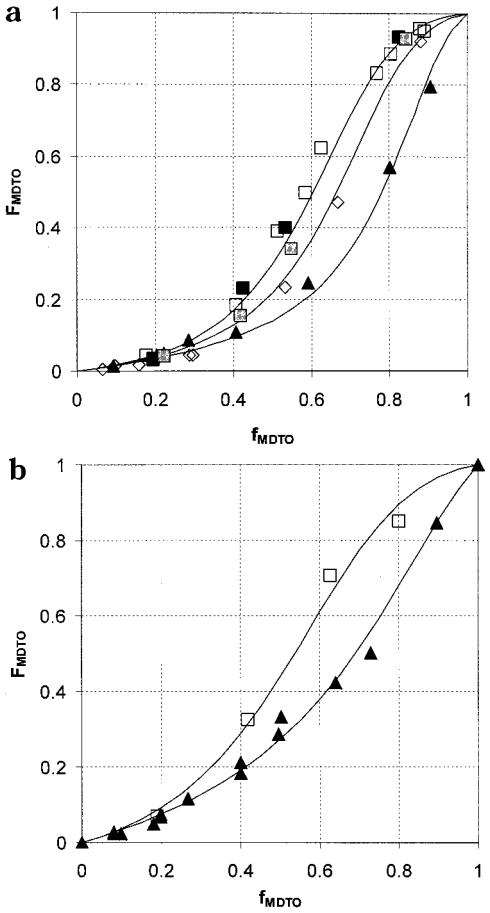

Figure 5. Copolymer composition plot showing the effect of dilution on the copolymer compositions of (a) STY−MDTO and (b) MMA−MDTO. Triangles, bulk; diamonds, 20 wt % solution in benzene; squares, 10 wt % solution in benzene (open squares), THF (black), or ^{t}BuOH (gray). Solid lines show the values predicted by the reversible cross-propagation model as discussed in the text.

Effect of Dilution. Changes in monomer concentration have a pronounced effect on the copolymer composition. Figure 5a shows the effect of dilution on the composition of MDTO−STY copolymers at 60 °C. A similar, though smaller effect was found for MMA (Figure 5b). The lower magnitude of the effect is ascribed in part to the faster rate of homopropagation for polymeric MMA radicals compared to that for STY radicals. It may also be due to a possible slower depropagation reaction (eq 3) for MDTO−MMA-terminated radicals compared to MDTO−STY-terminated radicals.

Effect of Changing Solvent. To exclude the possibility that the observed composition changes with dilution were the result of a solvent effect, MDTO−STY copolymerizations were performed in solution in THF and ^{t}BuOH. Copolymerizations in THF gave identical results to those carried out in benzene. Copolymerizations in ^{t}BuOH contained slightly lower levels of MDTO than the THF and benzene results but remained significantly different than the bulk polymerization. It seems likely that there is some solvent effect on the results of the ^{t}BuOH polymerizations (^{t}BuOH is a fairly poor solvent for poly(MDTO)) but that this is superimposed on an effect which is independent of the solvent used and depends purely on the monomer concentration (as shown by the THF/benzene results). These results are shown in Figure 5a. Composition data for these experiments are given in Table S1 of the Supporting Information.

Fit to Model. We attempted to fit the data for STY−MDTO and MMA−MDTO to the model described above. In this model, the reactivity ratios (r_1 and r_2) were presumed to be independent of temperature, while k_{-12}/k_{22} was allowed to vary with temperature. Table 2 shows the best fits of the model to the observed data for STY and MDTO. Graphical depictions of the model fits to styrene and MMA are shown in Figures 4 and 5.

As can be seen from the figures, the model developed in this paper fits the observed data both qualitatively and quantitatively, accounting for the changes in composition due to both dilution and temperature with the addition of a single temperature-dependent parameter, representing the ratio of the rate of homopropagation of the non-MDTO monomer (k_{22} in eq 5) and the rate of depropagation of MDTO (k_{-12} in eq 3). The small deviations that remain may be due to experimental errors in determining the copolymer compositions or may represent an oversimplification in the model. The success of the model in predicting the behavior of the system over a range of temperatures and concentrations, however, indicates that it is a valid basis for description of copolymerizations of MDTO.

Penultimate Unit Effect. The analysis above has neglected the possibility of an explicit penultimate unit effect. However, such effects may well take place, at least for STY-ended polymer radicals, as an MDTO−STY radical may show quite different reactivity to a STY−STY radical. Because of the length of the MDTO repeat unit (8 atoms, vs 2 for STY), however, it is unlikely that there will be a significant penultimate unit effect on MDTO-capped radicals. In this situation, the model described above may be extended to produce the following equation:

$$\frac{d[M_1]}{d[M_2]} = \frac{\langle r_1 \rangle f_1^{\,2} + f_1 f_2}{f_1 f_2 + \bar{r}_2 f_2^{\,2}} \tag{8a}$$

in which

$$\langle r_1 \rangle = r_1 \frac{f_2 + f_1/\bar{r}_2 + \dfrac{k_{-12}}{k_{22}([M_1]+[M_2])}}{f_2 + f_1/\bar{r}_2} \tag{8b}$$

and

$$\bar{r}_2 = r_2\left(\frac{f_1 + r_2 f_2}{f_1 + r'_2 f_2}\right) \tag{8c}$$

Equation 8 has essentially the same form as eq 6 based on the terminal model, except that r_2 is now replaced by the term $\bar{r}_2$, and k_{-12}/k_{22} becomes k_{-12}/k_{122}. The quality of the data obtained in these experiments is not sufficient to discriminate between these two models.

Sequence Distributions. The length of the MDTO repeat unit limits the amount of information that is available regarding sequence distribution in MDTO copolymers. As a result, the only information that can be obtained is the ratio of M_2−MDTO units to MDTO−MDTO units, where M_2 represents the comonomer. This is obtained from the ratio of vinylidene hydrogen peaks corresponding to each species. This information is sufficient, however, to determine the mean MDTO sequence length, which is equivalent to ($A_{MDTO-MDTO}$ +

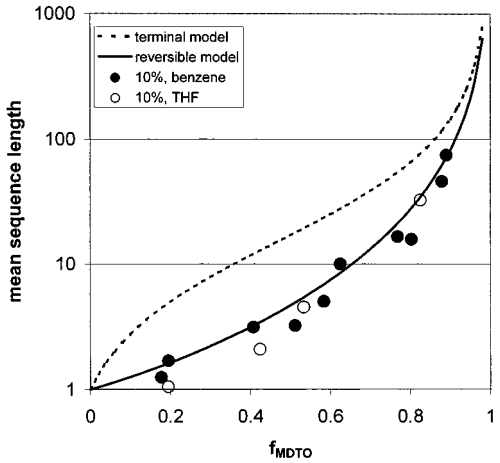

Figure 6. Experimentally observed variation in number-average MDTO sequence length in STY−MDTO copolymerizations with mole fraction MDTO in feed, compared to the predicted sequence length according to the terminal model ($r_1 = 8$, $r_2 = 16$, dotted line) and the reversible cross-propagation model ($r_1 = 0.06$, $r_2 = 7$, $k_{-12}/k_{22} = 17$, solid line). Points shown are 10 wt % solutions in benzene (filled circles) or THF (open circles).

$A_{M2-MDTO})/A_{M2-MDTO}$, where A_x represents the area of the peak corresponding to structure x. Comparison of the sequence lengths obtained with those predicted by the reversible cross-propagation model and the terminal model (with reactivity ratios adjusted to fit the composition data at each concentration) shows that, especially at low concentrations, the reversible cross-propagation model outlined in this paper produces a much better fit to the observed distribution (Figure 6) than does the terminal model.

Conclusions

MDTO is unusual among ring-opening monomers in that it readily forms copolymers with common acrylic and vinylic monomers such as methyl methacrylate and styrene. This apparent high reactivity is due to the reversibility of the addition reaction of MDTO radicals to double bonds. As this is the only reaction in the polymerization that is reversible, the net effect is an increase in the MDTO content of copolymers. The reversible cross-propagation model is supported by the variation of copolymer composition with monomer concentration and temperature, and the observed sequence distributions, as well as the ability of allylic sulfides to act as chain transfer agents.

The copolymer compositions of MDTO−STY and MDTO−MMA have been fitted to the reversible propagation model, yielding parameters (r_{MDTO}, r_2, k_{-12}/k_{22}) of (0.06, 7, 17) and (0.38, 3.2, 2.5), respectively, at 60 °C. The variation of the parameter k_{-12}/k_{22} with temperature has also been demonstrated, with the assumption that the reactivity ratios are independent of temperature between 25 and 80 °C.

Acknowledgment. We are grateful for the receipt of an Australian Postgraduate Reward for S.H. and funding from the Australian Research Council.

Appendix. Derivation of Reversible Cross-Propagation Copolymer Composition Equation

The copolymerization involves the following propagation and depropagation steps in addition to the standard initiation and termination steps:

propagation

$$M_1^\bullet + M_1 \rightarrow M_1^\bullet \qquad R_{11} = k_{11}[M_1^\bullet][M_1] \quad \text{(A1)}$$

$$M_1^\bullet + M_2 \rightarrow M_2^\bullet \qquad R_{12} = k_{12}[M_1^\bullet][M_2] \quad \text{(A2)}$$

$$M_2^\bullet + M_1 \rightarrow M_1^\bullet \qquad R_{21} = k_{21}[M_2^\bullet][M_1] \quad \text{(A3)}$$

$$M_2^\bullet + M_2 \rightarrow M_2^\bullet \qquad R_{22} = k_{22}[M_2^\bullet][M_2] \quad \text{(A4)}$$

depropagation

$$M_{12}^\bullet \rightarrow M_1^\bullet + M_2 \qquad R_{-12} = k_{-12}[M_{12}^\bullet] \quad \text{(A5)}$$

The species are designated by their usual symbols, with the subscript 1 representing MDTO and 2 the comonomer. $M_i^\bullet$ designates a polymeric radical whose terminal unit is designated by i. $M_{12}^\bullet$ represents a radical whose penultimate and ultimate units are MDTO and the comonomer, respectively. With the exception of the depropagation reaction, this species is assumed to undergo the same reactions as other $M_2^\bullet$ radicals.

Applying the steady-state assumption with regard to the total radical concentration, it is apparent that

$$\frac{-d[M_1]}{dt} = k_{11}[M_1^\bullet][M_1] + k_{21}[M_2^\bullet][M_1] \quad \text{(A6)}$$

$$\frac{-d[M_2]}{dt} = k_{12}[M_1^\bullet][M_2] + k_{22}[M_2^\bullet][M_2] - k_{-12}[M_{12}^\bullet] \quad \text{(A7)}$$

$$\frac{-d[M_{12}]}{dt} = k_{12}[M_1^\bullet][M_2] - k_{-12}[M_{12}^\bullet] - k_{22}[M_{12}^\bullet][M_2] - k_{21}[M_{12}^\bullet][M_1] \quad \text{(A8)}$$

$$\frac{-d[M_{12}]}{dt} = k_{12}[M_1^\bullet][M_2] - (k_{-12} + k_{22}[M_2] + k_{21}[M_1])[M_{12}^\bullet] \quad \text{(A9)}$$

Since $d[M_{12}^\bullet]/dt = 0$ (steady-state assumption),

$$[M_{12}^\bullet] = \frac{k_{12}[M_1^\bullet][M_2]}{(k_{-12} + k_{22}[M_2] + k_{21}[M_1])} \quad \text{(A10)}$$

Substituting into (A7),

$$\frac{-d[M_2]}{dt} = k_{12}[M_1^\bullet][M_2] + k_{22}[M_2^\bullet][M_2] - \frac{k_{-12}k_{12}[M_1^\bullet][M_2]}{(k_{-12} + k_{22}[M_2] + k_{21}[M_1])} \quad \text{(A11)}$$

$$= \frac{k_{22}[M_2] + k_{21}[M_1]}{(k_{-12} + k_{22}[M_2] + k_{21}[M_1])} k_{12}[M_1^\bullet][M_2] + k_{22}[M_2^\bullet][M_2]$$

$$\frac{d[M_1]}{d[M_2]} = \frac{k_{11}[M_1^\bullet][M_1] + k_{21}[M_2^\bullet][M_1]}{\frac{k_{22}[M_2] + k_{21}[M_1]}{k_{-12} + k_{22}[M_2] + k_{21}[M_1]} k_{12}[M_1^\bullet][M_2] + k_{22}[M_2^\bullet][M_2]} \quad \text{(A12)}$$

Now

$$\frac{-\mathrm{d}[M_2^\bullet]}{\mathrm{d}t} = k_{12}[M_1^\bullet][M_2] - k_{21}[M_2^\bullet][M_1] - k_{-12}[M_{12}^\bullet] \quad \text{(A13)}$$

$$= k_{12}[M_1^\bullet][M_2] - k_{21}[M_2^\bullet][M_1] - \frac{k_{-12}k_{12}[M_1^\bullet][M_2]}{(k_{-12} + k_{22}[M_2] + k_{21}[M_1])} \quad \text{(A14)}$$

$$= \frac{k_{22}[M_2] + k_{21}[M_1]}{(k_{-12} + k_{22}[M_2] + k_{21}[M_1])} k_{12}[M_1^\bullet][M_2] - k_{21}[M_2^\bullet][M_1] \quad \text{(A15)}$$

Since $\mathrm{d}[M_2^\bullet]/\mathrm{d}t = 0$ (steady-state approximation),

$$[M_2^\bullet] = \frac{\dfrac{k_{22}[M_2] + k_{21}[M_1]}{(k_{-12} + k_{22}[M_2] + k_{21}[M_1])} k_{12}[M_1^\bullet][M_2]}{k_{21}[M_1]} \quad \text{(A16)}$$

Substituting for $[M_2^\bullet]$ in (A12) and canceling $[M_1^\bullet]$s,

$$\frac{\mathrm{d}[M_1]}{\mathrm{d}[M_2]} = \left\{k_{11}[M_1] + \frac{k_{22}[M_2] + k_{21}[M_1]}{(k_{-12} + k_{22}[M_2] + k_{21}[M_1])k_{12}[M_1]}\right\} \Bigg/ \left\{\frac{k_{22}[M_2] + k_{21}[M_1]}{(k_{-12} + k_{22}[M_2] + k_{21}[M_1])} k_{12}[M_2] + k_{22}\frac{k_{22}[M_2] + k_{21}[M_1]}{(k_{-12} + k_{22}[M_2] + k_{21}[M_1])}\frac{k_{12}[M_2]^2}{k_{21}[M_1]}\right\} \quad \text{(A17)}$$

$$= \frac{[M_1]^2 + \dfrac{k_{22}[M_2] + k_{21}[M_1]}{(k_{-12} + k_{22}[M_2] + k_{21}[M_1])}\dfrac{k_{12}}{k_{11}}[M_2][M_1]}{\dfrac{k_{22}[M_2] + k_{21}[M_1]}{(k_{-12} + k_{22}[M_2] + k_{21}[M_1])}\left\{\dfrac{k_{12}}{k_{11}}[M_2][M_1] + \dfrac{k_{22}k_{12}[M_2]^2}{k_{21}k_{11}[M_1]}\right\}} \quad \text{(A18)}$$

This equation reduces to eq A19, using the standard definitions of r_1, r_2, f_1, and f_2 for the reactivity ratios and mole fractions of monomers 1 (M_1) and 2 (M_2).

$$\frac{\mathrm{d}[M_1]}{\mathrm{d}[M_2]} = \frac{r_1\dfrac{(k_{-12} + k_{22}[M_2] + k_{21}[M_1])}{k_{22}[M_2] + k_{21}[M_1]}f_1^2 + f_1f_2}{f_1f_2 + f_2^2} \quad \text{(A19)}$$

This expression is similar to the expression for the instantaneous copolymer composition according to the terminal model:

$$\frac{\mathrm{d}[M_1]}{\mathrm{d}[M_2]} = \frac{r_1f_1^2 + f_1f_2}{f_1f_2 + f_2^2} \quad \text{(A20)}$$

except that r_1 in eq A20 has been replaced with $r_1(k_{-12} + k_{22}[M_2] + k_{21}[M_1])/(k_{22}[M_2] + k_{21}[M_1])$ in eq A19. Thus, application of eq A20 to this system will produce a measured estimate of r_1, $\langle r_1\rangle$, which is actually equal to

$$\langle r_1\rangle = r_1\frac{k_{-12} + k_{22}[M_2] + k_{21}[M_1]}{k_{22}[M_2] + k_{21}[M_1]} \quad \text{(A21)}$$

$$= r_1\frac{f_2 + f_1/r_2 + \dfrac{k_{-12}}{k_{22}([M_1] + [M_2])}}{f_2 + f_1/r_2} \quad \text{(A22)}$$

As the monomer concentration ($[M_1] + [M_2]$) decreases, $\langle r_1\rangle$ will become larger. The effect will also become important in situations where $k_{22} \ll k_{-12}$ and when r_2 and f_2 approach zero. The value of $\langle r_1\rangle$ is also dependent on the comonomer composition and will vary as the composition of the solution changes.

Expressions for the average rate coefficient of propagation, sequence distributions, and expressions incorporating a penultimate unit effect on the rate of propagation of the comonomer may be derived in a similar fashion and are found to be identical to the standard expressions except for the substitution of $\langle r_1\rangle$ for r_1 given in eq A22.

Supporting Information Available: Tables containing primary data for Figure 1 and Figures 4−6. This material is available free of charge via the Internet at http://pubs.acs.org.

References and Notes

(1) Klemm, E.; Schulze, T. *Acta Polym.* **1999**, *50*, 1.
(2) Evans, R. A. *Chem. Aust.* **1996**, 83.
(3) Endo, T.; Yokozawa, T. In *Free-Radical Ring-Opening Polymerization*; Mijs, W. J., Ed.; Plenum: New York, 1992; pp 155−77.
(4) Moszner, N.; Zeuner, F.; Voelkel, T.; Rheinberger, V. *Macromol. Chem. Phys.* **1999**, *200*, 2173.
(5) Evans, R. A.; Rizzardo, E.; Moad, G.; Thang, S. H. *Macromolecules* **1994**, *27*, 7935.
(6) Evans, R. A.; Rizzardo, E. *Macromolecules* **1996**, *29*, 6983.
(7) Evans, R. A.; Rizzardo, E. *J. Polym. Sci., Part A: Polym. Chem.* **2001**, *39*, 202.
(8) Bailey, W. J. N.; Zhende, W.; Shang, R. *J. Polym. Sci., Polym. Chem. Ed.* **1982**, *20*, 3021.
(9) Roberts, G. E.; Coote, M. L.; Heuts, J. P. A.; Morris, L. M.; Davis, T. P. *Macromolecules* **1999**, *32*, 1332.
(10) Takahashi, T. *J. Polym. Sci., Part A-1* **1970**, *8*, 739.
(11) Sanda, F.; Takata, T.; Endo, T. *Macromolecules* **1994**, *27*, 3982.
(12) Miyagawa, T.; Sanda, F.; Endo, T. *J. Polym. Sci., A: Polym. Chem.* **2000**, *38*, 1861.
(13) Endo, T.; Kanda, N. *J. Polym. Sci., Polym. Chem. Ed.* **1985**, *23*, 1931.
(14) Harrisson, S.; Davis, T. P.; Evans, R. A.; Rizzardo, E. *Macromolecules* **2000**, *33*, 9553.
(15) Evans, R. A.; Rizzardo, E. *Macromolecules* **2000**, *33*, 6722.
(16) Coote, M. L.; Zammit, M. D.; Willett, G. D.; Davis, T. P. *Macromolecules* **1997**, *30*, 8182.
(17) *Contour:* van Herk, A. M. Available from the author: Laboratory of Polymer Chemistry, Eindhoven University of Technology, PO Box 513, 5600 MB Eindhoven, The Netherlands, 1996.
(18) Brandrup, J.; Immergut, E. H.; Grulke, E. A. *Polymer Handbook*, 4th ed.; Wiley-Interscience: New York, 1999.
(19) Yamada, B.; Saya, T.; Ohya, T.; Otsu, T. *Makromol. Chem.* **1982**, *183*, 963.
(20) Seno, M.; Kawamura, K.; Sato, T. *J. Polym. Sci., Part A: Polym. Chem.* **1996**, *34*, 3121.
(21) Sato, T.; Miki, K.; Seno, M. *Macromolecules* **1999**, *32*, 4166.
(22) Ito, O.; Matsuda, M. *J. Am. Chem. Soc.* **1979**, *101*, 5732.
(23) Ito, O.; Matsuda, M. *J. Am. Chem. Soc.* **1979**, *101*, 1815.
(24) Ito, O.; Matsuda, M. *Bull. Chem. Soc. Jpn.* **1978**, *51*, 427.
(25) Coote, M. L.; Davis, T. P. *Prog. Polym. Sci.* **1999**, *24*, 1217.
(26) Meijs, G. F.; Rizzardo, E.; Thang, S. H. *Macromolecules* **1988**, *21*, 3122.
(27) Barton, D. H. R.; Crich, D. *J. Chem. Soc., Perkin Trans. 1* **1986**, 1613.

MA0020584